COBEM2015

23rd ABCM International Congress of Mechanical Engineering
December 6-11, 2015, Rio de Janeiro, RJ, Brazil

NUMERICAL/ EXPERIMENTAL METHODOLOGY FOR SIMULTANEOUS DETERMINATION OF THERMAL PROPERTIES AND INTERNAL TEMPERATURE OF INDUSTRIAL EQUIPMENT

Bruno Henrique Oliveira Mulina
Solidônio R. de Carvalho
Valério Luiz Borges
Laboratório de Transferência de Calor e Massa - LTCM
brunomulina@gmail.com
srcarvalho@mecanica.ufu.br
vlborges@mecanica.ufu.br

Abstract. *The measurement and analysis of temperature in machinery and electric motors is an excellent tool for industrial maintenance. However, the majority of industrial equipment, such as: bearings and hydraulic pumps, do not have thermal sensors internally installed. Therefore, it is common to measure the temperature on accessible regions of the equipment, such as the external surface. However it is known that external temperature depends on the environment and the internal heat source, which may cause uncertainty in the measurement. In order to determine the internal temperature of industrial equipment, this work proposes the development of a numerical-experimental technique based on a non-invasive method. The technique is based on transient one-dimensional thermal model, inverse problems in heat transfer and experimental data to estimate thermal properties and determine internal temperature of industrial equipment. The proposed technique was evaluated with simulated experiments and comparisons with data from scientific literature. The results obtained demonstrated the feasibility and potential of the technique proposed in this work.*

Keywords: *Temperature, thermal properties, inverse problems, motors and bearings*

1. INTRODUCTION

The performance and life-cycle of electric motors and bearings can be monitored through temperature variations. The control of such parameter identifies ideal operating conditions, as shown by Cui *et al*. (2012), Bonnett (2001) e Y. Huai *et al*. (2003).

Matzan (2007) describes the use of thermography for the thermal monitoring of bearings in full operation, showing that the temperature increase is related to stanchion wear and reduced live-cycle of lubricants. Copper Alliance (2013) states that transformers with high-energy efficiency generate minimum heat. A similar phenomenon occurs in fuel cells, as described by Begot e Kauffmann (2008).

Several authors propose the use of thermal models to predict the internal temperature of equipment. With the use of a thermal model for an electric motor, Souza (2011) predicts the determination of operational failures, such as short-circuit and overload of the motor. Begot and Kauffmann (2008) uses inverse methods and temperature measurement to predict the temperature of fuel cells to provide higher performance and increased life-cycle. However, the thermal model strongly depends on the thermal properties of the component parts of the motor or fuel cell, these properties are sometimes unknown. Accordingly, it is necessary to use efficient techniques for determining the thermal properties of the materials involved. Borges (2008) proposes a non-destructive numerical/experimental technique for the simultaneous determination of thermal conductivity and diffusivity materials. The author makes use of experimental data, thermal modeling and techniques of inverse problems to achieve the proposed objectives.

Therefore, this paper proposes the development of a technique for determining the internal temperature of industrial equipment. The proposed method also has the advantage of estimate the thermal properties of the equipment's frame, from experimental parameters measured in situ, on the external surface of the machine. The technique combines low computational cost and agility in obtaining the data of interest.

2. DEVELOPMENT

There is a need to develop a technique that allows to obtain the internal temperature of industrial equipment quickly, simply and precisely. In this sense, this paper proposes the development of a noninvasive technique that involves modeling, optimization and the design of an experimental methodology to identify the variables of interest. The technique consists of estimating, simultaneously, conductivity and thermal diffusivity of the instrumented equipment, as well as to define its internal temperature, based on the following principles: Basically, we propose the following steps: 1) Thermal Modeling; 2) Instrumentation; 3) Estimation of thermal properties, temperature and internal heat flow. The developed technique aims instrumentation bearings, motors, hydraulic pumps and furnaces.

2.1. THERMAL MODELING

Figure 1a shows a scheme of the thermal problem to be studied. This is a theoretical model, corresponding to the real problem, in which ϕ_h represents the heat flow dissipated to the frame of the equipment by convection and / or radiation, ϕ_i the flow of internal heat generated by the device itself, and the variable of interest T_i , i.e., the internal temperature.

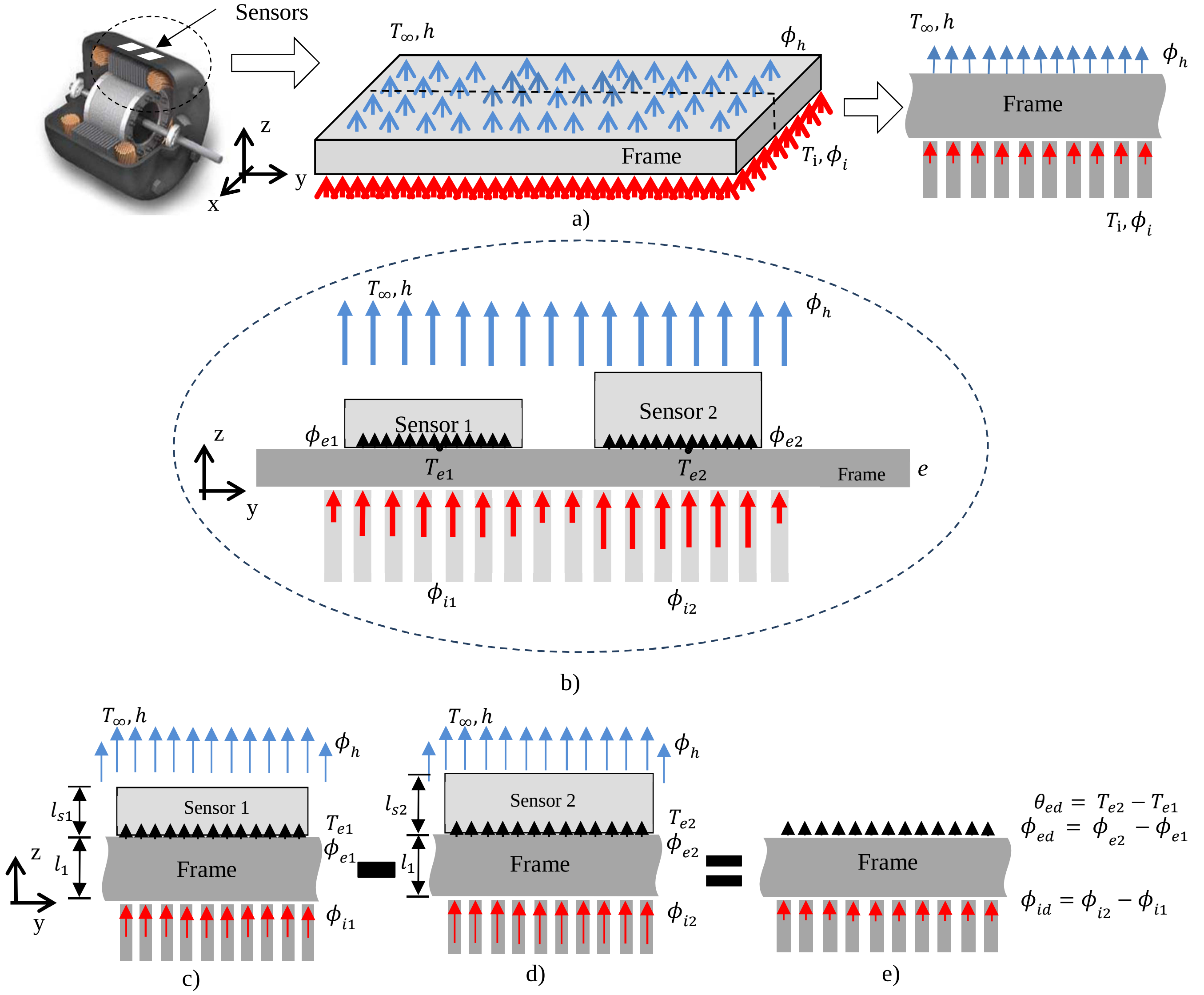

Figure 1. Equivalent thermal model for two thermal sensors. a) General thermal problem: the engine heat dissipation; b) 2D model with thermal sensors installed in the housing. c) Thermal problem Sensor 1; d) Thermal problem Sensor 2; e) Thermal problem "Difference Model".

The heat problem is presented in Fig. 1a in which it presents to the motor frame subjected to the boundary conditions of the internal heat flow type supplied by the motor, and heat losses by convection and radiative means to the external surface. The proposed technique consists in installing two sensors on the external surface of the frame, as seen in Fig. 1b. The sensors were developed especially for the technique in order to measure the temperature and heat flow on the outer wall of the frame. Each sensor highlighted in Fig. 2, is composed of a heat flux transducer, a thermocouple and a cover. What differentiates the sensors is the thickness of coverage in each of them.

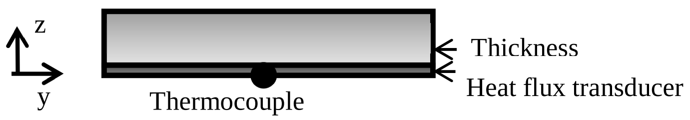

Figure 2. Scheme of thermal sensors.

The installation of the thermal sensors of different thickness alter locally the thermal exchanges between the frame and the environment, as presented in Fig. 1b. Because the sensors have different thicknesses, temperature and heat flows at the contact interface between the sensor and the frame vary. The same reasoning applies to the internal heat flow in the region below the sensors, as highlighted in Fig. 1b. The thermal variations caused by the presence of the sensors can be treated as one-dimensional and such behavior can be proved by means of computer simulations. Due to the presence of the cover on the flow and temperature sensors, heat exchange between the frame and the environment changes, this defines the sensor as active.

As the temperature at any point is defined by the overlap of the effects of initial temperature and by influences of the conditions applied to the faces (Beck, 1992), it is possible to admit that, subtracting the influences of each boundary condition obtained for the one-dimensional thermal models presented by Sensors 1 and 2, described in Figs. 1c and 1d, it is possible to define a third one-dimensional thermal problem, shown in Fig. 1e. The model, called "Difference Model", described by Eq. (1) can be resolved from information about the thermal properties of the frame, differences between the heat flows and the temperatures measured at the outside surface of the frame (ϕ_{ed} and θ_{ed}), and the difference between the heat flows in the internal surface the frame (ϕ_{id}). It should be noted that the use of "Difference Model" has the advantage of eliminating influences relating to thermal exchanges by convection and radiation between the outer surface and the environment.

$$\frac{\partial^2 T}{\partial z^2} = \frac{1}{\alpha}\frac{\partial T}{\partial t} \tag{1}$$

$$T(z,0) = 0$$

$$-k\left.\frac{\partial T}{\partial z}\right|_{z=0} = \phi_{id}(t) = \phi_{i2}(t) - \phi_{i1}(t)$$

$$-k\left.\frac{\partial T}{\partial z}\right|_{z=l_1} = \phi_{ed}(t) = \phi_{e2}(t) - \phi_{e1}(t)$$

The variation of temperature in the frame can be calculated from the one-dimensional heat diffusion equation (Eq. 2.1) subjected to internal and external boundary conditions. However, in real problems involving motors, bearings and others, both the thermal properties of the frame as the internal heat flow are generally unknown parameters.

3. CASE STUDY: SIMULATED EXPERIMENTS WITH PVC AND STEEL SAMPLES

In order to validate the technique, two simulated experiments were produced. The first consisted of analyzing the performance in a frame with low thermal conductivity of polyvinyl chloride (PVC). In the second, it was decided to evaluate the performance on a frame with superior thermal conductivity, in the case, the AISI 304 steel. The choice of such materials was based on extensive scientific literature, which reports its thermal properties. For the simulated experiments, solved the direct problem considering the one-dimensional models presented in Figs. 1c and 1d, which differ primarily by the thickness of sensors attached to the outer wall of the casing and thus heat flow imposed on the inner wall ($\phi_{i1} \neq \phi_{i2}$). The other boundary conditions and initial are similar.

In the first experiment were assigned values for ϕ_{i1} and ϕ_{i2} concerning the heat flow inside a PVC frame. In the second experiment, it was considered a metal frame of AISI 304 steel and new values for ϕ_{i1} and ϕ_{i2} The Tab. 1 shows the thermal properties of the frame and other conditions adopted in simulated experiments. In the process of calculation, the thermal contact resistance between the sample and sensor were despised and adjustments have been made with respect to thermal convection, duration of each experiment, time step, since they are frames with very different thermal properties.

It is noteworthy that for the calculation of thermal properties of the frame, especially the thermal diffusivity, the sensors cannot be in thermal equilibrium with the frame. The sensitivity of the technique is directly related to variations in heat flow and temperature monitored on the outer wall of the frame, immediately after the installation of the sensors. After knowing the thermal properties, the internal temperature of the frame can be estimated in a transient or steady state.

Table 1. Parameters applied to simulated experiments

Sensors			
Material		Copper	
Thermal diffusivity $[m^2/s]*10^6$		117	
Thermal conductivity $[W/mK]$		401	
Thickness sensor 1 [mm]		5	
Thickness sensor 2 [mm]		10	
Samples			
Material		PVC	Steel
Thermal diffusivity $[m^2/s]*10^7$		1,24	39,5
Thermal conductivity $[W/mK]$		0,16	14,9
Thickness (e) [mm]		0,025	0,01
Experimental data			
Heat flux	ϕ_{i1} [W/m^2]	150	2000
	ϕ_{i2} [W/m^2]	200	2500
Convection coefficient (h)		30	20
Acquisition interval [s]		1	1
Duration [s]		10000	500
Number of point		10000	500
Ambient Temperature [ºC]		25	25

The Figs. 3 and Fig. 4 present the temperatures T_{e1} and T_{e2}, and heat fluxes ϕ_{e1} and ϕ_{e2} calculated in the external part of the frame, as the solution of the direct problem for frames of PVC and AISI 304 steel in transient state.

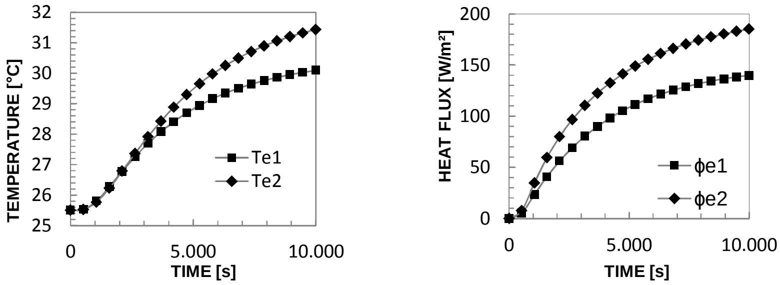

a) b)

Figure 3. First simulated experiment. Simulated data for PVC frame: a) Temperatures T_{e1} and T_{e2}. b) Heat fluxes ϕ_{e1} and ϕ_{e2} and the outer surface of the frame.

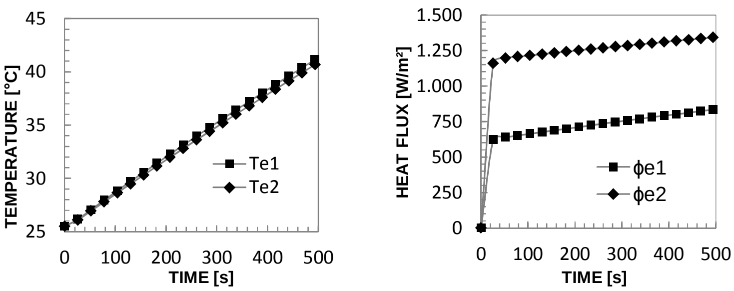

a) b)

Figure 4. Second simulated experiment. Simulated data for steel frame: a) Temperatures T_{e1} and T_{e2}. b) Heat fluxes ϕ_{e1} and ϕ_{e2} and the outer surface of the frame.

Figure 5 and Fig. 6 shows the results for the "Difference Model", i.e. the differences between the temperatures and heat flow measured at the outside surface of the frame (θ_{ed} and ϕ_{ed}) according to the simulated experiments for PVC and for steel AISI 304.

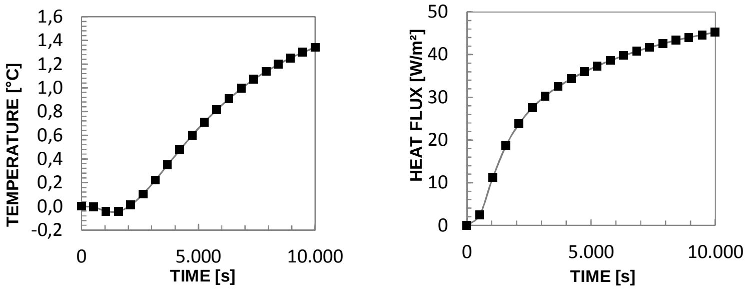

Figure 5 – Differences between the signals applied to PVC. a) Temperature $\theta_{ed}(t)$. b) Heat flux $\phi_{ed}(t)$.

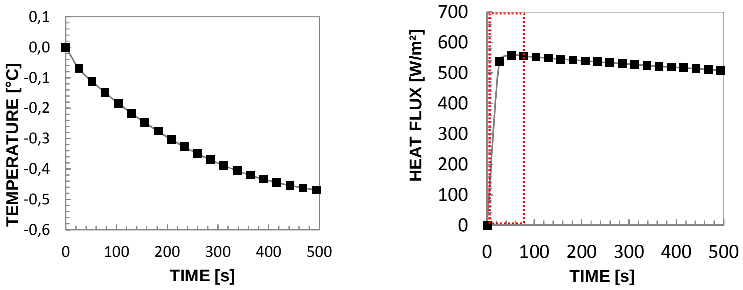

Figure 6 – Differences between the signals applied to steel. a) Temperature $\theta_{ed}(t)$. b) Heat flux $\phi_{ed}(t)$.

In the case of the experiment involving AISI 304 steel, it is noted that the external heat flow, $\phi_{ed}(t)$, tends rapidly to the permanent state. Therefore, to estimate the diffusivity in the metal frame, it was considered only the initial 50 seconds of the experiment, time interval in which there was greater variation in heat flux output.

4. RESULTS

4.1. ESTIMATE OF THERMAL PROPERTIES

The technique consists in estimating simultaneously the thermal diffusivity (α) of the frame and the internal heat flow $\phi_{id}(t)$ imposed to the difference model. Shortly thereafter, the thermal conductivity (k) is estimated and the internal temperature of the frame.

Through the analysis of the transient thermal problem shown in Eq. (1), it is noted the linear dependency between thermal properties α and k. Accordingly, the thermal diffusivity α is estimated using a dynamic model to be applied to the thermal problem. According to Borges (2008), the thermal problem described in Eq. (1) in the time domain can be transformed by means of the Fourier transform, in a dynamic system in the frequency domain, as shown in Eq. (2). This equation is called Generalized Impedance and is defined by the relationship between the output signals and input signals respectively represented by the temperature and heat flux signals applied to the heat problem. In this case, according Borges (2008), the thermal diffusivity may be estimated exclusively by analyzing the phase of the dynamic system.

The technique considers that the internal heat flow, ϕ_{id}, unknown, will be constant throughout the solution of the thermal problem. This simplification makes, from the Fourier transform, this parameter be null. Therefore, Eq. (2) can be simplified by making the dynamic model dependent on only the data obtained on the outer surface, i.e., θ_{ed} and ϕ_{ed}.

$$Z_d(f) = \frac{Y(f)}{X(f)} = \frac{\theta_{ed}(f)}{\phi_{ed}(f) - \phi_{id}(f)} = \frac{\theta_{ed}(f)}{\phi_{ed}(f)} = |Z_d(f)| e^{j\,\varphi_d(f)} \qquad (2)$$

Basically, the technique for estimating the thermal diffusivity begins in the time domain, however, it is completed in the frequency domain. The problem is resolved direct in the time domain by imposing 25 values for the internal heat flow, ϕ_{id}, between zero and the largest predicted experimental value in W/m² and 25 values for thermal diffusivity α ranging from 10^{-10} and 10^{-4} m²/s. The thermal conductivity is assumed constant and has a unitary value.

Because it is a one-dimensional thermal problem, it took only 200 cells to ensure the convergence of the numerical solution in the time domain. The computational cost was relatively low, i.e., about 12 minutes to generate the response surface for the experiment involving the PVC frame and 27 seconds for the metallic frame. The computational algorithm was developed in MatLab and calculations were performed on a desktop with an I5 processor with 4GB RAM.

After the solution of the heat problem, it is applied the Fourier transform to the response surface to obtain a set of corresponding values $Z_{d\_calc}(f)$ to the response surface (θ_{ed} and ϕ_{ed}). Furthermore, it is calculated $Z_{d\_exp}(f)$

corresponding to the previous data obtained through the simulated experiment (Fig. 6). As mentioned by Borges (2008) for calculating the thermal diffusivity, it is necessary only to analysis of the dynamic model $Z_d(f)$. Accordingly, by means of a least squares function defined by the relationship between $\varphi_d(\phi_{ide\_exp}, \alpha_{exp})$ (phase calculated from experimental data) and $\varphi_d(\phi_{id\_calc}, \alpha_{calc})$ (phases calculated from the response surface) you can analyze the root mean square error E_φ between experimental and calculated data, as shown in Eq. (3).

$$E_\varphi = \sum_{i=1}^{N} \left(\varphi_d(\phi_{ide\_exp}, \alpha_{exp}) - \varphi_d(\phi_{id\_calc}, \alpha_{calc})\right)^2 \quad (3)$$

The Fig. 7a and Fig. 8a shows the values of E_φ for experiments with PVC and steel AISI 304, respectively. The lighter region in the figures identifies the location where the E_φ function assumes the maximum value for each type of frame. In a complementary way, Fig. 7b and Fig. 8b shows the sensitivities E_φ with respect to the ϕ_{id} term denominated as $S_{E_\varphi,\phi_{id}}$, for each kind of frame. Furthermore, Fig. 7c and Fig. 8c present the sensitivity E_φ for the termα, named $S_{E_\varphi,\alpha}$.

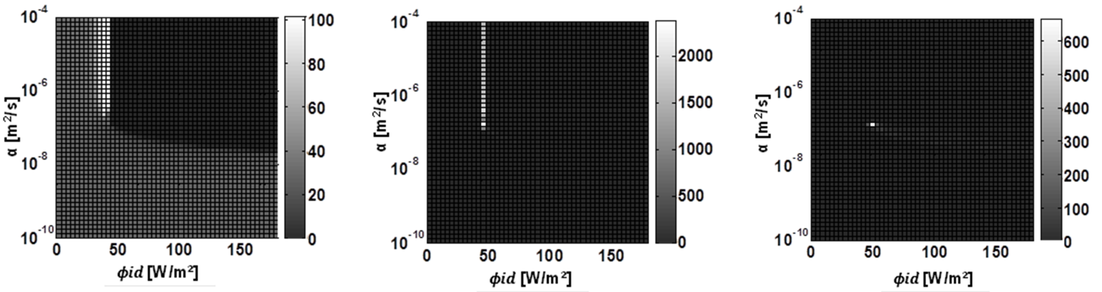

a) b) c)

Figure 7. Study from E_φ to experiment with PVC. a) E_φ. b) $S_{E_\varphi,\phi_{id}^*}$. c) S_{E_φ,α^*}.

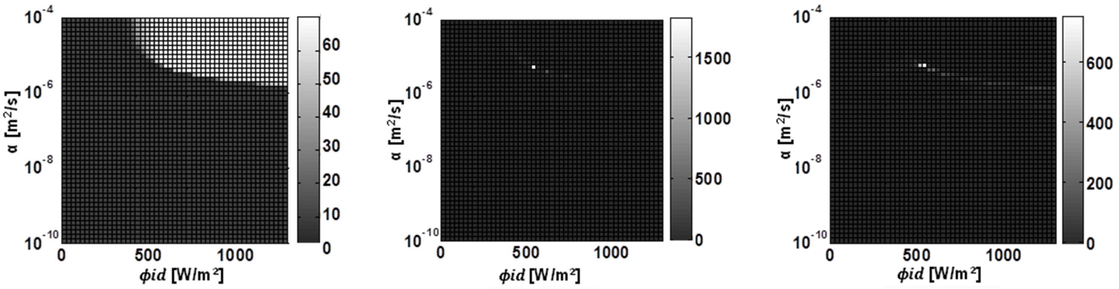

a) b) c)

Figure 8. Study from E_φ to experiment with steel. a) E_φ. b) $S_{E_\varphi,\phi_{id}^*}$. c) S_{E_φ,α^*}.

The Fig. 7b and Fig. 7c, and Fig. 8b and Fig. 8c confirm the existence of values for ϕ_{id} and α values for which the sensitivity E_φ acquires maximum value: lighter points in the figures. Thus, one can restrict the analysis of the problem to a specific range of values of ϕ_{id} and α, i.e.: $48 \le \phi_{id} \le 60$ and $5 \cdot 10^{-8} \le \alpha \le 5 \cdot 10^{-7}$ (for PVC) and $320 \le \phi_{id} \le 540$ and $2 \cdot 10^{-6} \le \alpha \le 5 \cdot 10^{-6}$ (for the steel AISI304). Fig. 9 shows α and E_φ values obtained for the range of heat fluxes defined by sensitivity. It is possible to identify the optimal values of ϕ_{id} and α that result in the least global value of the E_φ within this range. By applying the optimization for Golden Section Method (Vanderplaats, 1986), the values of α that minimize E_φ can be estimated.

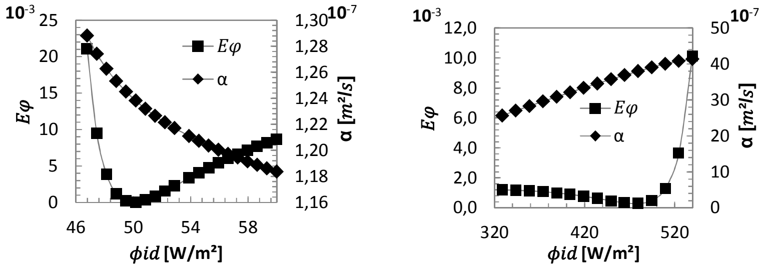

a) b)

Figure 9. Great values ϕ_{id} and α resulting in minimum overall value of E_φ. a) PVC. B) Steel

After the optimal values of ϕ_{id} and α are applied in the "Difference Model" on the time domain (Eq. 1) and again applying the Golden Section Method with cubic polynomial approximation, the thermal conductivity k is estimated for the PVC and steel frames. For each experiment simulated, there is only one variable to be determined, i.e., k which is estimated by minimizing a square minimum function E_k as Eq. (4). In the equation θ_{ed} it represents the experimental temperature and θ_{cd} the temperature calculated by the thermal problem. As conditions boundary, it is used the heat flux ϕ_{ed} measured experimentally on the face x=L of the "Difference Model", and heat flow ϕ_{id}, at x=0, previously estimated in the later step, together with the thermal diffusivity.

$$E_k = \sum_{t=1}^{N} (\theta_{ed}(t) - \theta_{cd}(t))^2 \quad (4)$$

The Tab. 2 shows the values obtained for the thermal properties using the proposed technique and difference model. In addition, it presents the absolute error between the values applied in simulated experiments and in those estimated.

Table 2. Comparison between experimental and calculated thermal properties.

		Experiment	
		PVC	Steel
Thermal diffusivity $[m^2/s]*10^7$	Applied	1,24	39,5
	Estimated	1,2336	39,47
	Error (%)	0,535%	0,08%
Thermal conductivity $[W/mK]$	Applied	0,16	14,9
	Estimated	0,1736	15,9
	Error (%)	8,5%	6,71%

4.2. TEMPERATURE AND INTERNAL HEAT FLOW CALCULATION

With the thermal properties of the frame known, it is possible to estimate the heat flow in the inner wall of the frame ϕ_i, the heat transfer coefficient by convection h and finally the inner temperature of the frame T_i.

To estimate the internal heat flux ϕ_i and the h there is the need to simultaneous resolve the thermal problems shown in Fig. 2c and 2d. To estimate ϕ_i the one-dimensional thermal models consider only the frame subject to the following boundary conditions (Eqs. (5) to (8)):

$$-k\left.\frac{\partial T}{\partial z}\right|_{z=0} = \phi_{i1} = \phi_i \quad (5)$$

$$-k\left.\frac{\partial T}{\partial z}\right|_{z=e} = \phi_{e1} \quad (6)$$

$$-k\left.\frac{\partial T}{\partial z}\right|_{z=0} = \phi_{i2} = \phi_i + \phi_{id} \quad (7)$$

$$-k\left.\frac{\partial T}{\partial z}\right|_{z=e} = \phi_{e2} \quad (8)$$

To estimate the heat transfer coefficient h by convection, the thermal one-dimensional models consider only the sensors and their respective thicknesses subjected to the following boundary conditions defined by Eqs. (9) to (12).

$$-k\left.\frac{\partial T}{\partial z}\right|_{z=l_1} = \phi_{e1} \quad (9)$$

$$-k\left.\frac{\partial T}{\partial z}\right|_{z=l_{s1}} = h(T - T_\infty) \quad (10)$$

$$-k\left.\frac{\partial T}{\partial z}\right|_{z=l_1} = \phi_{e2} \quad (11)$$

$$-k\left.\frac{\partial T}{\partial z}\right|_{z=l_{s2}} = h(T - T_\infty) \quad (12)$$

The value of ϕ_i and h are estimated separately by means of techniques of inverse problems applied to heat transfer problems. In this case, from the Golden Section method, is minimized for each thermal problem the S function, as described in Eq. (13), which makes use of experimental temperatures T_{e1_exp} and T_{e2_exp} measured by the sensors and temperatures T_{e1_calc} and T_{e2_calc} calculated on the external surface as the models described in Figs. 2.1c and 2.1d.

$$S = \sum_{t=1}^{N} \left[\left(T_{e1\_exp}(t) - T_{e1\_calc}(t) \right)^2 + \left(T_{e2\_exp}(t) - T_{e2\_calc}(t) \right)^2 \right] \quad (13)$$

Table 3 shows the internal heat flows ϕ_{i1} and ϕ_{i2} obtained for each thermal problem, and the error between the experimental values and the calculated by the proposed technique.

Table 3. Comparison between experimental and estimated internal heat fluxes.

		Experiment	
		PVC	Steel
ϕ_{i1} [W/m^2]	Applied	150	2000
	Estimated	152,54	2071,42
	Error (%)	3,03%	3,571%
ϕ_{i2} [W/m^2]	Applied	200	2500
	Estimated	202,6	2565,42
	Error (%)	1,3%	2,63%

As reported earlier, the parameters ϕ_{i1} and ϕ_{i2} are influenced by the sensors positioned on the external surface of the frame. Therefore, to finally calculate the ϕ_i value, it becomes appropriate to adopt a weighted function that relates the thickness of the sensors and the estimated flux according to Eq. (14). Thus, it is obtained a more consistent estimate of the internal heat flux ϕ_i for a instrumented region.

$$\phi_i\ (t) = \frac{l_1 * \phi_{i1} + l_2 * \phi_{i2}}{l_2 + l_1} \quad (14)$$

The value of heat transfer coefficient by convection is estimated presented in Table 4.

Table 4. Comparison between experimental and estimated convective coefficient.

	Experiments	
	PVC	Steel
Applied	30	30
Estimated	30,4	28,5
Error (%)	3,4%	5%

After knowing all boundary conditions and thermal properties, it is finally estimated the inner temperature of the frame by means of the solution of the direct thermal problem shown in Fig. 2.1a. The Fig. 10a and Fig. 11a show the comparison between the experimental temperatures T_{e1} and T_{e2}, and calculated T_{c1} and T_{c2} at the interfaces between the frame and the sensors 1 and 2, according to the experiments involving PVC and steel, respectively. The Fig. 10b and Fig. 10b present the internal temperatures for each type of frame and the corresponding experimental values. Finally, Fig. 10c and Fig. 11c shows the errors between the experimental and calculated values.

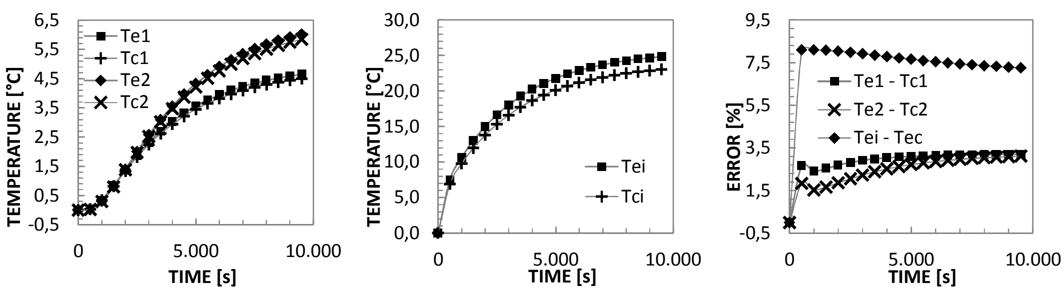

a) b) c)

Figure 10. Temperatures obtained for PVC. a) In the interface. b) Internal. c) Relative error.

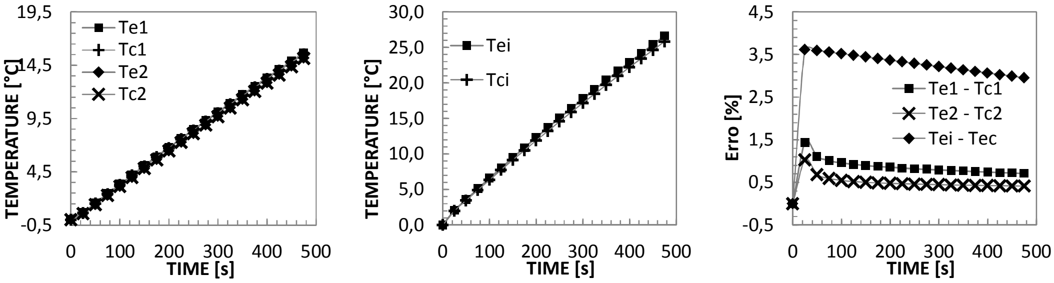

a) b) c)

Figure 11. Temperatures obtained for steel. a) In the interface. b) Internal. c) Relative error.

4. CONCLUSIONS

This paper presents a numerical/experimental technique for determination of thermal properties and internal temperature of industrial equipment

From the definition of the thermal problem, design of auxiliary thermal problems, experimental data, use of a Difference Model and techniques of inverse problems in heat transfer, it was estimated the variables of interest from two simulated experiments.

By means of analyzing the results, it was noted a good consistency between the simulated and experimental data, which confirmed the potential and feasibility of use of the technique for insulating and metallic materials.

Based on the scientific literature, it appears that the majority of techniques available makes use of samples and controlled laboratory experiments for estimating simultaneously the thermal properties of materials. The advantage of this technique compared to others is the possibility of its use in the field, directly on the material being studied.

Finally, it is considered that the present work took just one step forward to the great challenge that is to determine simultaneously the thermal properties and internal temperature of industrial equipment. Experiments are being prepared in the laboratory to confirm the viability and further enhance the technical proposal.

5. ACKNOWLEDGEMENTS

The authors thank the funding agencies CAPES, CNPq and FAPEMIG, and the Graduate Program in Mechanical Engineering from the institutional and financial support.

6. REFERENCES

BECK, J. V., COLE, K. D., HAJI-SHEIKH, A., LITKOUHI, B. Heat Conduction Using Green's Functions. Hemisphere Publishing Corporation, Washington D. C, USA. 1992.

BÉGOT, S.; KAUFFMANN J.M. Estimation of internal fuel cell temperatures from surface temperature measurements.
Journal of Power Sources, v. 178, n. 1, p. 316-322, mar. 2008.

BONNETT, A.H. Operation temperature consideration and performance characteristics for IEEE 841 Motors. IEEE Transactions on Industry Applications. vol. 37, n. 4, p.1120-1131, ago. 2001.

BORGES, V. L.. Desenvolvimento do método de aquecimento plano parcial para a determinação simultânea de propriedades térmicas sem o uso de transdutores de fluxo de calor. 2008. 129 f. Tese de Doutorado. Universidade Federal de Uberlândia, Uberlândia, Uberlândia.

COPPER ALLIANCE. Temperature Rise and Transformer Efficiency. Disponível em: <http://www.copper.org/environment/sustainable-energy/transformers/education/trans_efficiency.html>. Acesso em 10/02/2013.

CUI, Y.; WU, G.; Gao, G.; Luo, Y.; Cao, K. Analysis and Calculation of Three-dimensional Temperature Field of Inverter-fed Traction Motor. Journal of Modern Mathematics Frontier, vol. 1, n. 1, p.1-5. 2012

HUAI, Y.; MELNIK, R.V.N.; THOGERSEN, P.B. Computational analysis of temperature rise phenomena in electric induction motors, Applied Thermal Engineering, vol. 23, n. 7, p. 779-795, mai. 2003.

MATZAN, E. Detecting Premature Bearing Failure. Machinery Lubrication Magazine, mai. 2007. Disponível em: <http://www.machinerylubrication.com/Read/1041/detecting-bearing-failure>. Acesso em: 2 jan. 2012

SOUSA, K. M.. VALIDAÇÃO DE MODELO TÉRMICO E ELÉTRICO DE MOTOR DE INDUÇÃO EMPREGANDO REDES DE BRAGG EM FIBRA ÓTICA. 122 f. Dissertação de Mestrado, Universidade Tecnológica Federal do Paraná. Pato Branco, 2011.

7. RESPONSIBILITY NOTICE

The authors are the only responsible for the printed material included in this paper.